Measurement of the high-frequency electro-optical Kerr effect in a plastic crystal: Succinonitrile

T. Bischofberger* and E. Courtens
IBM Zurich Research Laboratory, 8803 Rüschlikon-ZH, Switzerland
(Received 3 September 1976)

The nonlinear Kerr susceptibility of an oriented succinonitrile single crystal has been measured throughout the cubic plastic phase. The measurement procedure is described in detail, and the results discussed in terms of an orientational correlation function. Connection with other measurements is also made.

I. INTRODUCTION

The high-frequency electro-optical Kerr effect has been extensively studied in isotropic media, but relatively little is known about this property in anisotropic media. It has been shown that the effect can be fairly large in molecular crystals composed of optically anisotropic molecules having considerable reorientational freedom (plastic crystals).[1] In succinonitrile, pretransitional behavior on the approach of the plastic-solid and plastic-liquid phase transitions has also been observed.

The electric-field-induced birefringence contains direct information on the strength of the orientational correlation of the molecules.[2] The same information can be obtained from the integrated strength of the depolarized light-scattering spectra.[3] But in general, owing to the weakness of the scattered light, absolute intensity measurements tend to be inaccurate so that there is a definite advantage in measuring the Kerr effect.

The measurement techniques have been well-developed for isotropic media[4] and the present paper will indicate in detail how one can proceed to obtain components of the Kerr tensor in anisotropic media, with particular application to the cubic plastic phase of succinonitrile. Attention will be restricted to the case where there is a strong orienting field at frequency ω_0 and a weak probing field at a different frequency ω_p with $|\omega_0 - \omega_p| \gg 1/\tau$, where τ is a typical value of the molecular reorientation time. In this case the nonlinear Kerr susceptibility tensor $\bar{\bar{\chi}}^{\mathrm{NL}}$ is defined in terms of the dielectric tensor $\bar{\bar{\epsilon}}$ by

$$P_i = \epsilon_{ij} E_j = \epsilon_p E_i + 4\pi \chi^{\mathrm{NL}}_{ijkl} \langle F_k F_l \rangle E_j , \qquad (1)$$

where P_i is a component of the polarization vector, ϵ_p is the linear dielectric constant at the frequency of the probing field $\vec{E}$, and $\vec{F}$ is the (real) orienting field. The bracket is an average over the optical period, so that for a linearly polarized field, $\vec{F}$ can simply be replaced by the field amplitude divided by $\sqrt{2}$. The nonlinear susceptibility tensor $\chi^{\mathrm{NL}}_{ijkl}$ is symmetric in the first and last pair of indices and reflects the symmetry of the medium. The indices should not be confused with some other definitions of the nonlinear susceptibility which are obtained either when $\vec{E}$ and $\vec{F}$ are not distinct or when the field vectors are complex.

With $\vec{E}$ and $\vec{F}$ distinct, the measurement of $\epsilon^{\mathrm{NL}}_{ij}$ is similar to that of the Cotton-Mouton effect (the magneto-optical analog of the electro-optical Kerr effect). The dependence on crystal orientations in the latter case has been investigated recently in great detail by Pisarev *et al.*[5] The case of cubic crystals is contained in that description but is given again in Sec. II to clarify the notation and to point to the approximations involved. The expressions obtained in Sec. II are those that were used for the original Kerr measurements on succinonitrile.[1] Section III describes the experimental arrangement and results on succinonitrile. Section IV is a discussion of these results making connections with other measurements as well as with theoretical interpretations.

II. DEPENDENCE ON CRYSTAL ORIENTATION

As is well-known, induced birefringence measurements on cubic crystals only yield the components $\chi^{\mathrm{NL}}_{1111} - \chi^{\mathrm{NL}}_{1122}$ and $\chi^{\mathrm{NL}}_{1212}$. To obtain $\chi^{\mathrm{NL}}_{1111}$ independently would require an absolute measurement of the refractive index. In the case where $\vec{E}$ and $\vec{F}$ in Eq. (1) are the same frequency ω, that information could also be obtained from ellipse-rotation measurements as known for isotropic media.[6] In this case the connection between $\bar{\bar{\chi}}^{\mathrm{NL}}(\omega, \omega)$ and $\bar{\bar{\chi}}^{\mathrm{NL}}(\omega_p, \omega_0)$ has to be treated carefully as pointed out by Gires and Paillette.[7] The present descriptions will be restricted to distinct fields $\vec{E}$ and $\vec{F}$ and thus to the measurement of $\chi^{\mathrm{NL}}_{11} - \chi^{\mathrm{NL}}_{12}$ and χ^{NL}_{44} only (from now on the abbreviated subscript notation is used, i.e., $\chi^{\mathrm{NL}}_{1111} = \chi^{\mathrm{NL}}_{11}$, $\chi^{\mathrm{NL}}_{1122} = \chi^{\mathrm{NL}}_{12}$ and $\chi^{\mathrm{NL}}_{1212} = \chi^{\mathrm{NL}}_{44}$). The most useful crystal cut to this effect is the $(1\bar{1}0)$ plane as shown in Fig. 1. For this particular orientation the nonlinear part of the dielectric tensor $\bar{\bar{\epsilon}}$ is

$$\vec{\vec{\epsilon}}^{\,NL} = 4\pi F^2 \begin{bmatrix} [\chi_{11}^{NL} a^2 + \chi_{12}^{NL}(a^2+c^2)] & 2\chi_{44}^{NL} a^2 & 2\chi_{44}^{NL} ac \\ 2\chi_{44}^{NL} a^2 & [\chi_{11}^{NL} a^2 + \chi_{12}^{NL}(a^2+c^2)] & 2\chi_{44}^{NL} ac \\ 2\chi_{44}^{NL} ac & 2\chi_{44}^{NL} ac & [2\chi_{12}^{NL} a^2 + \chi_{11}^{NL} c^2] \end{bmatrix} , \tag{2}$$

where $a = (1/\sqrt{2})\sin\theta$, $c = \cos\theta$ with the orienting field $\vec{F} = F[a, a, c]$. θ is the angle between the $[0, 0, 1]$ axis and the direction of the orienting field $\vec{F}$.

To obtain the depolarized Kerr signal it is necessary to solve the eigenvalue problem $\vec{\vec{\epsilon}}^{NL}\vec{X}_i = 4\pi F^2 \lambda_i \vec{X}_i$ leading to the principal axes $\vec{X}_i$ of the nonlinear dielectric tensor and the corresponding eigenvalues λ_i. One finds on the basis of symmetry

$$\vec{X}_1 = (1/\sqrt{2})[1, -1, 0] . \tag{3a}$$

Solving the remaining 2×2 problem one has

$$\vec{X}_{2,3} = S[-2\chi_{44}^{NL} ac, -2\chi_{44}^{NL} ac, \sqrt{2}\,\lambda_1 - \lambda_{2,3} + 4\chi_{44}^{NL} a^2] , \tag{3b}$$

where S is the appropriate normalization. The corresponding eigenvalues are

$$\lambda_1 = (1\sqrt{2})[(\chi_{11}^{NL} + \chi_{12}^{NL} - 2\chi_{44}^{NL})a^2 + \chi_{12}^{NL} c^2] , \tag{4a}$$

$$\lambda_{2,3} = \tfrac{1}{2}[\sqrt{2}\,\lambda_1 + 2(\chi_{12}^{NL} + 2\chi_{44}^{NL})a^2 + \chi_{11}^{NL} c^2 \pm \sqrt{R}] , \tag{4b}$$

with

$$R = [\sqrt{2}\,\lambda_1 - 2(\chi_{12}^{NL} - 2\chi_{44}^{NL})a^2 - \chi_{11}^{NL} c^2]^2 + 32(\chi_{44}^{NL})^2 a^2 c^2 . \tag{4c}$$

For the given probing field (Fig. 1), $\vec{E} = [(1/\sqrt{2}) \times \sin(\theta + \pi/4), (1/\sqrt{2})\sin(\theta + \pi/4), \cos(\theta + \pi/4)]$ and a phase lag much smaller than a quarter wave, the relative depolarized Kerr signal is easily calculated using Eqs. (3) and (4):

$$\frac{I_{dep}}{I_p} = \frac{(E_2 E_3)^2}{|\vec{E}|^4}\left(\frac{\pi l}{\lambda_p}\right)^2 (\delta n_2 - \delta n_3)^2 , \tag{5}$$

where $E_{2,3} = \vec{E} \cdot \vec{X}_{2,3}$ are the projections of $\vec{E}$ on the principal axes $\vec{X}_{2,3}$, l is the thickness of the material and λ_p is the vacuum wavelength of the probing field. $(\delta n_2 - \delta n_3)$ is the difference between the induced changes in the refractive index. Since the induced anisotropy is small, the difference between the propagation direction of the ordinary and extraordinary rays has been neglected. For the same reason $\delta\epsilon_{2,3} = 2n_{2,3}\delta n_{2,3} = \lambda_{2,3}$ or $\delta n_{2,3} = \lambda_{2,3}/2n_p$, where n_p is the refractive index at the probing wavelength. The square of the difference in the refractive indices is thus

$$(\delta n_2 - \delta n_3)^2 = (4\pi^2 F^4/n_p^2)(\lambda_2 - \lambda_3)^2 = (4\pi^2 F^4/n_p^2)R. \tag{6}$$

Finally, the relative Kerr signal will be

$$\frac{I_{dep}}{I_p} = 4\pi^4 \frac{l^2}{\lambda_p^2}\frac{F^4}{n_p^2}(\chi_{11}^{NL} - \chi_{12}^{NL})^2[1 - \zeta_\alpha(1 + 6\cos^2\theta)\sin^2\theta]^2 . \tag{7a}$$

ζ_α is the anisotropy of the nonlinear susceptibility tensor $\vec{\vec{\chi}}^{NL}$ (later referred to as the orientational anisotropy),

$$\zeta_\alpha = \tfrac{1}{2} - \chi_{44}^{NL}/(\chi_{11}^{NL} - \chi_{12}^{NL}) . \tag{7b}$$

Note that in the isotropic phase (liquid phase) the relation $\chi_{11}^{NL} - \chi_{12}^{NL} - 2\chi_{44}^{NL} = 0$ gives zero anisotropy.

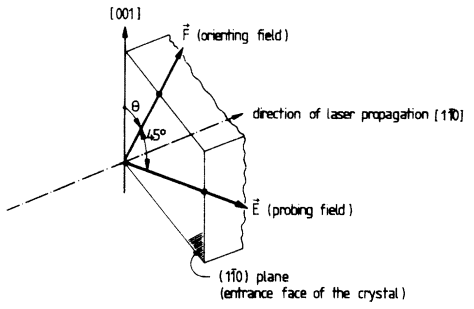

FIG. 1. Geometry of the high-frequency electro-optical Kerr-effect experiment.

III. EXPERIMENT

The experimental arrangement is shown in Fig. 2. The value of the nonlinear susceptibility $(\chi_{11}^{NL} - \chi_{12}^{NL})$ was measured using a single transverse (TEM_{00}) and longitudinal mode, Q-switched, pulsed ruby laser ($\lambda_0 = 6943$ Å) as orienting field $\vec{F}$ and its second harmonic generated in a $LiIO_3$ crystal ($\lambda_p = 3472$ Å) as probing field $\vec{E}$.

The use of a single-mode laser is necessary for these measurements since one cannot allow for unknown field fluctuations occurring in times short compared to the reorientational relaxation time. In addition, single-mode operation provides for much better pulse-to-pulse reproducibility. The monochromaticity of the laser was checked with high-resolution Fabry-Perot exposures. Occasional operation on two nearby modes occurred and appeared as a beat in the time evolution of the pulse. These shots were eliminated from the data.

The beams are linearly polarized at 45° from

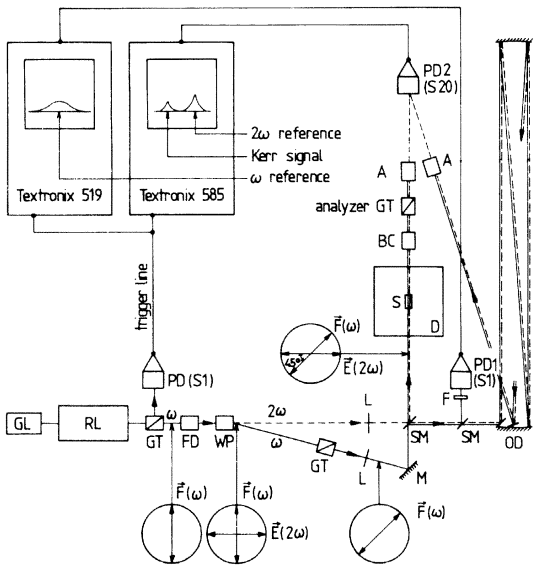

FIG. 2. Schematic diagram of the experimental set-up. The direction of polarization of the probing and orienting fields is indicated in the large open circles. GL: He-Ne laser, used for alignment; RL: pulsed ruby laser; GT: Glan-Thompson polarizer; PD: photodiode; FD: frequency doubler; WP: Wollaston prism; L: lens; M: mirror; SM: semi-transparent mirror; F: red transmitting filter; OD: optical delay line; D: dewar with sample S; BC: Berek compensator; A: $CuSO_4$ solution.

one another, superposed, and incident perpendicular to a $(1\bar{1}0)$ cut of an 8-mm-long crystal.[8] The probing field is then passed through a Berek compensator and an analyzer, and is finally detected with a fast UV-sensitive photodiode. The compensator is carefully adjusted so that no depolarized signal is observed in the absence of the orienting field. After passing through the crystal, the orienting field is absorbed in a 2-cm-thick saturated $CuSO_4$ solution. Reference signals of the probing and orienting fields are recorded simultaneously with the Kerr signal seen in Fig. 3.

The reference signal of the orienting field was detected on a fast oscilloscope. Kerr signal and optically delayed reference signal of the probing field were recorded on a slower oscilloscope. Since the pulse duration of ~30 nsec is much longer than the orientational relaxation times, the depolarized Kerr signal was measured at pulse peak.

The crystal was mounted in a thermostatic holder between two thin Schlieren free quartz windows. Good optical quality was achieved by using a few drops of octane on the crystal surface for refractive-index matching. The sample could be rotated around the beam direction and the measurements were repeated for various angles θ. The temperature of the holder could be stabilized within 0.01 °C.

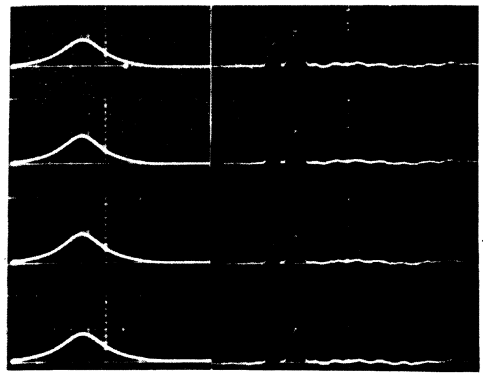

FIG. 3. Oscilloscope traces at a fixed orientation from four successive laser shots. On the left, the laser signal on the photodiode PD 1 (20 nsec/div) and on the right, Kerr signal followed by the reference signal on the photodiode PD 2 (50 nsec/div).

A relative calibration of the measurement of $(\chi_{11}^{NL} - \chi_{12}^{NL})$ was made against CCl_4 whose induced birefringence is well-known, $(\chi_{11}^{NL} - \chi_{12}^{NL}) = (1.00 \pm 0.04) \times 10^{-13}$ cm^3/erg at 23 °C.[9] The absolute calibration was done by measuring the ruby-laser power P_0, the power ratio P_{dep}/P_p of the Kerr signal and of the reference signal, the beam cross sections at the sample and the beam divergences for the probing and orienting fields. The two calibrations led to the same Kerr susceptibility of our succinonitrile sample within the experimental uncertainty.

To be able to relate the quantities measured in the experiment to the nonlinear tensor components $(\chi_{11}^{NL} - \chi_{12}^{NL})$, Eq. (7) is modified so that the power ratios actually measured do appear. For TEM_{00} Gaussian beams with $1/e^2$ intensity radii W_p and W_0, the probing and orienting radial intensities are

$$I_p(r) = (cn_p/4\pi)E^2 \exp(-2r^2/W_p^2) \tag{8a}$$

and

$$I_0(r) = (cn_0/4\pi)F^2 \exp(-2r^2/W_0^2)\ , \tag{8b}$$

respectively.

The normalized expression for the angular dependence of the Kerr signal is

$$\frac{P_{dep}}{P_p P_0^2} = \frac{g}{\lambda_p^2 c^2 \epsilon_p \epsilon_0} (\chi_{11}^{NL} - \chi_{12}^{NL})^2 f(\theta) \tag{9a}$$

with

$$f(\theta) = [1 - \zeta_\alpha(1 + 6\cos^2\theta)\sin^2\theta]^2\ . \tag{9b}$$

ϵ_p and ϵ_0 are the optical-dielectric constants for the probing and orienting fields, respectively,

and g is a geometrical factor with the dimensions of an inverse area $g = 64\pi^2 l^2/(W_0^4 + 2W_0^2 W_p^2)$. Equation (9) is only valid for phase lags much smaller than a quarter wave. To fulfill this condition for the entire range of the experiment, the orienting field had to be attenuated in the temperature region near the plastic-solid phase transition. The unattenuated beam energy was always kept small ($\sim 10^{-4}$ J) to avoid damage to the crystal as well as disturbing contributions from other nonlinearities.

Figure 4 shows a measurement at fixed temperature as a function of crystal orientation. Each point is the mean derived from four laser shots. The plot is normalized so that the ordinate is $f(\theta)$. The results are corrected for the relatively small window contribution, $(\chi_{11}^{NL} - \chi_{12}^{NL}) = 0.41 \pm 0.02 \times 10^{-13}$ cm^3/erg for fused quartz at room temperature.[10] The solid curve is given by Eq. (9b) and is obtained by a least-square fit of the normalization constant and ζ_α. A series of similar measurements, with six points between $\theta = 0$ and $\frac{1}{2}\pi$ was performed as a function of temperature. Typical results are shown in Fig. 5. The results close to melting cannot be plotted on this scale as they would strongly superimpose. The temperature dependence of the orientational anisotropy ζ_α is shown in Fig. 6, whereas a generalized susceptibility Q [proportional to $(\chi_{11}^{NL} - \chi_{12}^{NL})$ as explained in the following section] is given in Fig. 7. It should be emphasized that the remarkable decrease of ζ_α on the approach of T_M is not related to sample premelting. It is well-known that impure samples do melt locally below T_M, giving rise to strong opalescence and to a gradual decrease of all crystalline properties. This behavior was recently observed in succinonitrile in the course of a detailed refractive-index measurement.[11] However, no opalescence was observed in our excellent sample[8] up to a few tenths of °C from T_M. Furthermore, had opalescence occurred, this would also have strongly reduced the value of $(\chi_{11}^{NL} - \chi_{12}^{NL})$, and such a reduction is not seen.

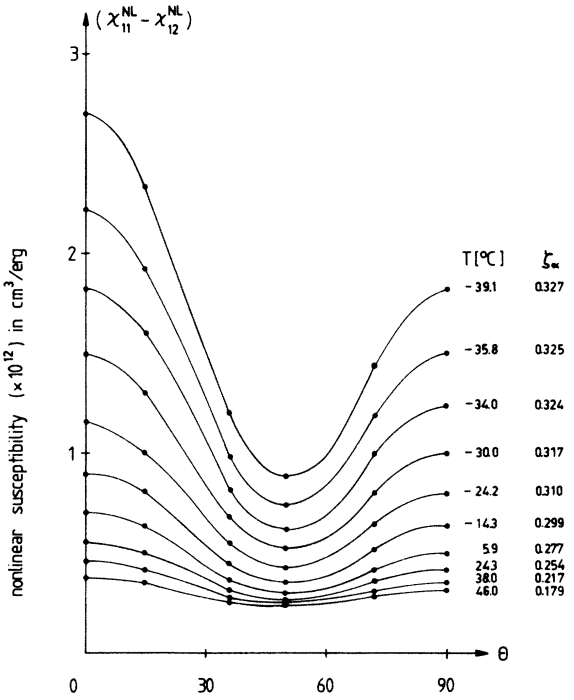

FIG. 5. The angular dependence of the nonlinear Kerr susceptibility $(\chi_{11}^{NL} - \chi_{12}^{NL})$ at different temperatures.

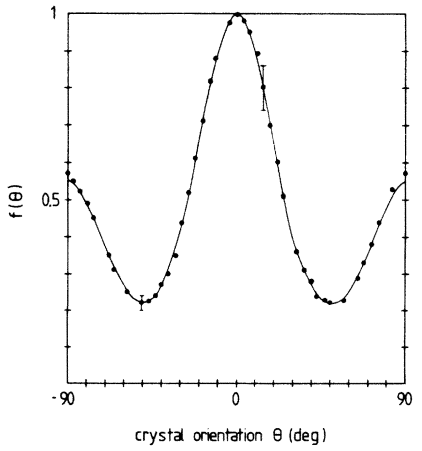

FIG. 4. The angular dependence of the normalized Kerr signal at 19.9 °C. The solid curve corresponds to Eq. (9b) with $\zeta_\alpha = 0.265$.

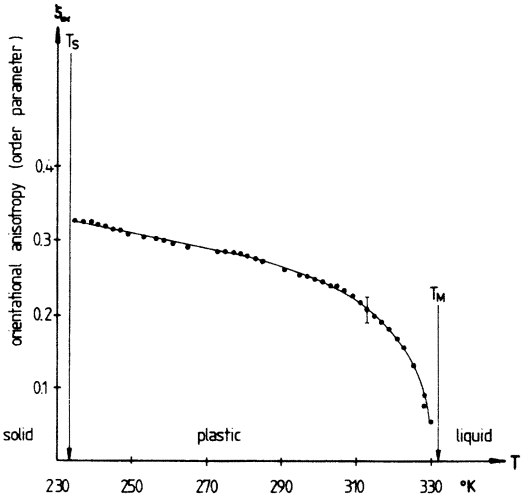

FIG. 6. The orientational anisotropy $\zeta_\alpha = \frac{1}{2} - \chi_{44}^{NL}/(\chi_{11}^{NL} - \chi_{12}^{NL})$ as a function of temperature. The solid curve is a guide to the eye.

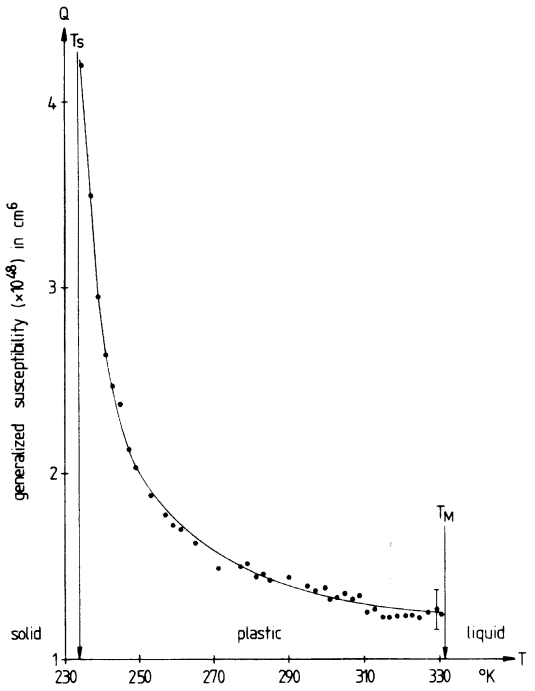

FIG. 7. The generalized susceptibility Q as a function of temperature. The solid curve is a guide to the eye.

IV. DISCUSSION

The nonlinear susceptibility $\tilde{\chi}^{NL}$ measured at frequencies below electronic absorption is the sum of several contributions. There is an electronic contribution (hyperpolarizability) that arises from the nonlinear distortions of the electron orbits. A so-called "nuclear" contribution arises from an electric-field-induced change in the relative position of the centers of mass; it can be thought of as nonlinear local field effects. If the molecules are optically anisotropic there is also an orientational contribution that arises from electric-field-induced changes in the molecular orientations. Finally, there is electrostriction which results from a modification of the overall density. Recent measurements[9] on CCl_4 and different glasses[10] have shown that the electronic part and the "nuclear" part are of the same order of magnitude in these systems, whereas in liquids with strongly optically anisotropic molecules, the orientational part (which appears with the same field dependence as the "nuclear" part) can be orders of magnitude larger than the first two contributions.[12] For short measuring times electrostriction can be made to play a minor role as it is associated with mass flow.

For the present interpretation of the Kerr susceptibility $\tilde{\chi}^{NL}$, it is assumed that the main nonlinearity arises from the orientational contribution. This seems justified from the order of magnitude of the effect measured as well as from its temperature dependence. Then $\tilde{\chi}^{NL}$ is related to a tensorial polarizability correlation function,[2] given by

$$\chi^{NL}_{ijkl} = N\beta L_0 L_p^2 G_{ijkl} \tag{10a}$$

with

$$G_{ijkl} = \frac{1}{2\mathfrak{N}} \sum_{a,b} \mathrm{tr}[\rho_0 A^a_{ij}(\omega_p) A^b_{kl}(\omega_0)], \tag{10b}$$

where N is the number of molecules per unit volume, $\mathfrak{N}$ is the total number of molecules in the sample, and $\beta = 1/k_B T$. The Lorentz-Lorenz factors are designated by $L_i = \frac{1}{3}(\epsilon_i + 2)$ for $i = 0$ or p. The traceless, second-rank tensor $A_{kl} = \alpha_{kl}(\omega) - \mathrm{tr}\rho_0 \alpha_{kl}(\omega)$ represents the anisotropic part of the molecular polarizability, where ρ_0 is the orientational distribution function containing all angular coordinates of the molecules. The trace (tr) represents symbolically an integration over all coordinates. $\tilde{G}(\omega_p, \omega_0)$ is an orientational-correlation function of the anisotropic part of the molecular polarizability. In a cubic crystal with four-fold symmetry, $\tilde{G}$ has only two independent components G_{1111} and G_{1212} (in the abbreviated subscript notations G_{11} and G_{44}) because $\tilde{A}$ is a traceless tensor and, therefore, the trace over the first two subscripts vanishes, leading to $G_{11} + 2G_{12} = 0$.

A group-theoretical analysis[2] of the tensorial-correlation function G shows that the tensor decomposes into two irreducible tensorial sets which are expressed by the two independent components of $\tilde{G}$,

$$G_{11} = \frac{1}{6\mathfrak{N}} \sum_{a,b} \mathrm{tr}\left[\rho_0 \sum_i^3 A^a_{ii} A^b_{ii}\right], \tag{11a}$$

$$G_{44} = \frac{1}{6\mathfrak{N}} \sum_{a,b} \mathrm{tr}\left[\rho_0 \sum_{i<j}^3 A^a_{ij} A^b_{ij}\right]. \tag{11b}$$

The first set transforms as the representation $\mathfrak{D}^{(0)}$ of the full rotation group and is proportional to $Q \equiv G_{11} + 2G_{44}$. The second set transforms as $\mathfrak{D}^{(4)}$, and is proportional to $C \equiv G_{11} - \frac{4}{3}G_{44}$.

The orientational correlation of molecular pairs a-b is a short-range property in the plastic phase. Correlated pairs contribute to Q, whether ρ_0 has cubic or spherical symmetry. In other words, Q will be different from zero both in the plastic and liquid phases. The correlation strength Q depends on the degree of orientational correlation of given pairs and on the number of pairs contributing to the sum in Eq. (11) which is the correlation range. Therefore, Q can be considered as a generalized susceptibility which is a measure of the short-range molecular ordering. It can be compared to the paramagnetic susceptibility of a magnet above

the Curie point, which measures the short-range spin ordering. The generalized susceptibility can be expressed in terms of the measured quantities $(\chi_{11}^{NL} - \chi_{12}^{NL})$ and ζ_α (Fig. 7):

$$Q(T) = k_B T(\chi_{11}^{NL} - \chi_{12}^{NL})(\tfrac{5}{3} - 2\zeta_\alpha)/NL_0L_P^2 . \qquad (12)$$

$N = A\rho/M$ is the number of molecules per unit volume expressed by Avogadro's number A, the mass density ρ, and the molecular weight M. The temperature dependence of the Lorentz-Lorenz factors L_0 and L_P were determined from the known refractive indices[11] throughout the plastic phase at the corresponding wavelengths.[13] The change in sample density with temperature was calculated from the linear expansion coefficient measured by x-ray diffraction[14] in the plastic phase. The increase in the number of vacancies with temperature was neglected. An upper limit to the vacancy concentration at the melting point can be obtained by comparison of the bulk and x-ray expansion coefficients[15] and leads to a concentration of 0.1 mole percent.

The dimensionless orientational anisotropy is related to $\bar{G}$ and $\bar{\chi}^{NL}$ by

$$\zeta_\alpha = \frac{C}{2G_{11}} = \frac{1}{2} - \frac{2}{3}\frac{G_{44}}{G_{11}} = \frac{1}{2} - \frac{\chi_{44}^{NL}}{\chi_{11}^{NL} - \chi_{12}^{NL}} . \qquad (13)$$

In the liquid phase, ζ_α and the related C are zero. The correlated molecular pairs contribute to C because of short-range correlation, but only to the extent that the orientational distribution function ρ_0 has cubic symmetry, which is a long-range property of the plastic phase. However, after division by G_{11} in Eq. (13) it appears that the orientational anisotropy ζ_α retains only the information about this cubic symmetry. If one assumes that the correlation range affects the off-diagonal and the diagonal elements of $\bar{A}^a$ and $\bar{A}^b$ in the same way in Eq. (11), the ratio G_{44}/G_{11} in Eq. (13) is independent of the short-range correlation. Therefore ζ_α measures the anisotropy of the orientational correlation of the molecules, i.e., a long-range property. It can be considered as an order parameter of the cubic phase. However this is not an order parameter in the usual sense, as it is a pair property.

If instead the sum in Eq. (11) were taken over all molecular pairs a-a only (self-correlation) ζ_α would measure the anisotropy of the average molecular orientation, and this would be a more usual orientational order parameter. Such an orientational order parameter could be measured by means of Raman light-scattering experiments.

However, within a mean-field theory and for rod-like molecules, the orientational anisotropy ζ_α is proportional to $(5\langle\cos^4\delta\rangle - 1)$, namely, to the average over the angular distribution function of the fourth-order spherical harmonics $P_4(\cos\delta)$. The angle between the molecular axis and a fourfold cubic axis is designated by δ. In contrast to liquid crystals, the average of $(3\langle\cos^2\delta\rangle - 1)$ is always zero in the present case of cubic symmetry. The order parameter ζ_α is thus a direct extension to higher-order spherical harmonics of orientational order parameters.[16] One might want to note that higher-order harmonics have also been measured in liquid crystals.[17] In the present case the considerable decrease of ζ_α near the melting temperature indicates that the molecular orientational correlation becomes more and more isotropic. The temperature dependence of ζ_α is similar to that found for the elastic anisotropy $\zeta_\epsilon = \frac{1}{2} - C_{44}/(C_{11} - C_{12})$.[18]

The results can also be related to recent depolarized light-scattering measurements.[19-21] In depolarized light scattering a reorientational Rayleigh wing is observed whose integrated intensity is proportional to the correlation function $\bar{G}$.[22] In addition to this wing one observes a broad depolarized background whose origin can tentatively be ascribed to librations. A careful comparison of the integrated intensity of the wings in different crystallographic directions leads, after subtraction of the broad background, to the same ζ_α as that reported in Fig. 6.[20] The full analysis is rather delicate and requires extensive numerical treatment of the data as the wing line width and the background intensities both depend on crystal orientation and temperature. These observations are at variance with a recent report by Boyer *et al.*[23] who found a temperature-independent value of ζ_α. We believe that the discrepancy arises from an improper handling of the background and of the linewidth in their evaluations.

V. SUMMARY AND CONCLUSIONS

The measurements of the nonlinear Kerr susceptibility and of the orientational anisotropy reveal a remarkable pretransitional behavior on the approach of the plastic-solid and plastic-liquid transition points. The measured nonlinear susceptibility tensor can be understood as a tensorial polarizability correlation function. A qualitative interpretation of this correlation function leads to the following results. Throughout the plastic phase the Kerr susceptibility is a measure of the short-range orientational molecular ordering. As the temperature is lowered towards the plastic-solid phase transition, molecular segments become correlated over longer distances. The considerable decrease of the orientational anisotropy near the melting point found by the Kerr effect[1]

and confirmed by light-scattering experiments[20] suggests that as the temperature is raised the orientational correlation of the molecules becomes more and more isotropic until melting occurs. However, this observed pretransitional effect can hardly be interpreted as the cause for melting. It should be noted that melting of succinonitrile is clearly a first-order transition as indicated by refractive-index measurements.[11] The loss of anisotropy in orientational correlation is not reflected by any curvature of the refractive index below the melting point, and thus there appears to be no coupling between ζ_α and the density.

ACKNOWLEDGMENT

The authors express their gratitude to Dr. H. Fontaine who supplied the oriented crystals and made results available before publication.

*Present address: Dept. of Physics, University of California, Lawrence Berkeley Laboratory, Berkeley, Calif. 94720.

[1]T. Bischofberger and E. Courtens, Phys. Rev. Lett. 32, 163 (1974).
[2]E. Courtens, Phys. Rev. A 10, 967 (1974).
[3]L. Boyer, R. Vacher, L. Cecchi, M. Adam, and P. Bergé, Phys. Rev. Lett. 26, 1435 (1971).
[4]P. D. Maker and R. W. Terhune, Phys. Rev. 137, A801 (1965).
[5]R. V. Pisarev, I. G. Sinii, N. N. Kolpakova, and Yu.M. Vakovlev, Sov. Phys.-JETP 33, 1175 (1971).
[6]P. D. Maker, R. W. Terhune, and C. M. Savage, Phys. Rev. Lett. 12, 507 (1964).
[7]F. Gires and M. Paillette, C. R. Acad. Sci. 267, B1153 (1968).
[8]Grown and oriented by H. Fontaine, University of Lille, 59-Villeneuve d'Ascq, France.
[9]R. W. Hellwarth, A. Owyoung, and N. George, Phys. Rev. A 4, 2343 (1971).
[10]A. Owyoung, R. W. Hellwarth, and N. George, Phys. Rev. B 5, 628 (1972).
[11]R. M. MacFarlane, E. Courtens, and T. Bischofberger, Mol. Cryst. Liq. Cryst. 35, 27 (1976).
[12]G. K. L. Wong and Y. R. Shen, Phys. Rev. A 10, 1277 (1974).
[13]L. Boyer, R. Vacher, M. Adam, and L. Cecchi, in *Proceedings of the Second International Conference on Light Scattering in Solids*, edited by M. Balkanski (Flammarion, Paris, 1971), p. 498.
[14]H. Fontaine and M. Bée, Bull. Soc. Fr. Mineral. Crystallogr. 95, 441 (1972).
[15]R. H. Baughman and D. Turnbull, J. Phys. Chem. Solids 32, 1375 (1971).
[16]R. L. Humphries, P. G. James, and G. R. Luckhurst, J. Chem. Soc. Faraday Trans. II, 68, 1031 (1972).
[17]S. Jen, N. A. Clark, P. S. Pershan, and E. B. Priestley, Phys. Rev. Lett. 31, 1552 (1973).
[18]H. Fontaine and C. Moriamez, J. Chim. Phys. Phys. Chim. Biol. 65, 969 (1968).
[19]T. Bischofberger and E. Courtens, Phys. Rev. Lett. 35, 1471 (1975).
[20]T. Bischofberger, Thesis (Swiss Federal Institute of Technology, Zurich, Switzerland, 1976) (unpublished).
[21]L. Boyer, R. Vacher, and L. Cecchi, J. Phys. (Paris) 36, 1347 (1975).
[22]E. Courtens, J. Phys. Lett. 37, L-21 (1976).
[23]L. Boyer, R. Vacher, J. P. Bonnet, and L. Cecchi, in *Proceedings of the Third International Conference on Light Scattering in Solids*, edited by M. Balkanski, S. P. S. Porto, and R. C. C. Leite (Flammarion, Paris, 1976), p. 702.

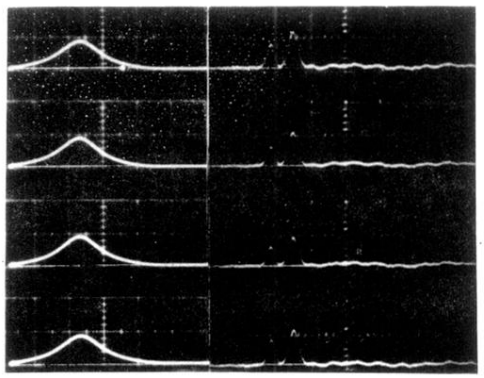

FIG. 3. Oscilloscope traces at a fixed orientation from four successive laser shots. On the left, the laser signal on the photodiode PD 1 (20 nsec/div) and on the right, Kerr signal followed by the reference signal on the photodiode PD 2 (50 nsec/div).